

Galaxy evolution at low redshift?

II. Number counts and optical identifications of faint IRAS sources

E. Bertin^{1,2}, M. Dennefeld^{1,3}, and M. Moshir⁴

¹ Institut d’Astrophysique de Paris, 98bis Boulevard Arago, F-75014 Paris, France

² Sterrewacht Leiden, PO Box 9513, 2300 RA Leiden, The Netherlands

³ Université Pierre & Marie Curie, 4, place Jussieu, F-75005 Paris, France

⁴ Infrared Processing and Analysis Center, California Institute of Technology, Pasadena, CA 91125, USA

Received 10 July 1996 / Accepted 20 November 1996

Abstract. We analyse a Far InfraRed (FIR) catalogue of galaxies at $60\ \mu\text{m}$ with a flux limit of ≈ 110 mJy, extracted from a deep subsample of the IRAS Faint Source Survey. Monte-Carlo simulations and optical identification statistics are used to put constraints on the evolution of galaxies in the FIR. We find evidence for strong evolution of IRAS galaxies, in luminosity $\propto (1+z)^{3.2 \pm 0.2 \pm 0.3}$ or density $\propto (1+z)^{6.0 \pm 0.5 \pm 0.7}$ for $f_\nu(60\ \mu\text{m}) > 150$ mJy, in agreement with previous claims. An excess of rather red faint optical counterparts with $B > 18$, consistent with the above evolution, is detected. We interpret these results as strong evolution at recent times among the starburst (or dusty AGN) population of merging/interacting galaxies. Most of these objects at moderate redshifts may pass unnoticed among the population of massive spirals in broad-band optical surveys, because of large amounts of dust extinction in their central regions. A possible link with the strong evolution observed in the optical for blue sub- M^* galaxies is discussed.

Key words: infrared: galaxies – galaxies: evolution – galaxies: starburst – galaxies: interactions – galaxies: fundamental parameters

1. Introduction

This is the second paper in a series where we try photometrically to quantify galaxy evolution at low redshifts ($z < 0.3$), from reasonably large and homogeneous samples. We have shown in Bertin & Dennefeld (1996, paper I) that optical galaxy counts were consistent with little evolution down to $B_J = 21$, corresponding to $z \approx 0.2$ for M^* galaxies. In this paper, we investigate the case of the far-infrared domain.

The Far-InfraRed (FIR) is very sensitive to ongoing star-formation activity in galaxies. Warm dust, essentially heated by

the blue/UV continuum of young OB stars, makes a large contribution to the total FIR output of late-type objects. At the same time, a significant heating by an Active Galactic Nucleus (AGN) is possible in the most luminous FIR-emitting objects, although the respective contributions of star-formation and AGNs are not yet well determined. In this context, a statistical analysis of a deep and homogeneous FIR-selected galaxy sample should easily allow one to trace evolution of star-formation and/or AGN activity with redshift.

The IRAS (InfraRed Astronomical Satellite) survey, with its four infrared channels at 12, 25, 60 and $100\ \mu\text{m}$ provides a unique tool for such studies, despite its moderate sensitivity. Based on the Point Source Catalog (PSC) and the more recent Faint Source Catalog (FSC) extracted from the IRAS data, several workers have investigated the evolution hypothesis on subsamples reaching various depths. The situation is still somewhat unclear, although evolution seems to be detected at $60\ \mu\text{m}$ in most cases. Using PSC data, with solid identifications and radial velocities, Saunders et al. (1990) claimed a very strong evolution effect in their sample, while Fisher et al. (1992) found theirs compatible with no evolution (the latter has however a somewhat lower median redshift). Using the deeper FSC data, Lonsdale et al. (1990) found evidence for strong evolution from source number counts. Oliver et al. (1995) reported also evolution in their spectroscopic subsample, though at a slightly milder rate. Two deeper studies (Hacking & Houck 1987 and Gregorich et al. 1995) made on much smaller specific areas (a few tens of square degrees) suggest a large excess of faint detections.

In order to clarify the problem and to complete these studies by providing the “missing link” between extensive, shallow catalogs ($f_\nu(60\ \mu\text{m}) > 0.2$ Jy) and small, very deep studies ($f_\nu(60\ \mu\text{m}) \lesssim 100$ mJy), we have undertaken an identification program of IRAS sources at $60\ \mu\text{m}$ on some selected areas in the sky, focusing ourselves especially on the faintest flux domain achievable with the Faint Source Survey (FSS) “plates”: $f_\nu(60\ \mu\text{m}) \approx 120$ mJy with a signal-to-noise ratio of 4. Our purpose is twofold: (1) to estimate the reliability of the IRAS

Send offprint requests to: E. Bertin (*bertin@iap.fr*)

Table 1. IRAS fields

Field	α (2000.0)		δ (2000.0)		Area (sq. degrees)
	h	m	°	'	
N1	09	20	+78	20	80.8
N2	15	25	+55	00	113.5
N3	17	50	+47	30	83.2
S	03	50	-47	00	133.7

survey at its very faint end, and (2), to characterize the population of IRAS galaxies in the 100 mJy domain (where evolution is expected to begin to show up in models of FIR galaxy counts).

At this low S/N level, the data cannot be interpreted in a straightforward way: completeness, reliability and measurement biases must be quantified accurately. We rely here on both Monte-Carlo simulations and optical identifications to estimate these effects.

The paper is organized as follows. In Sect. 2 we describe the selection of the infrared “real” sample. Sect. 3 is devoted to the description of our Monte-Carlo simulations of IRAS catalogs. These are then used in Sect. 4 to interpret statistics on the infrared data (confusion noise, number counts). In Sect. 5 we rely on optical identifications to put further constraints on the nature of faint sources. We summarize our results in Sect. 6 and compare them to those of other studies. In Sect. 7, we finally discuss the implications in the framework of galaxy evolution.

2. The data

The data in this study come from the Very Faint Source Sample (VFSS). The VFSS was generated by one of us (MM) after the completion of the FSS. The data in the FSS were searched for regions where 1) The IR cirrus indicators NOISRAT and NOISCOR (Moshir et al. 1992) were small, 2) the spacecraft coverage was at least 4 HCONs and 3) there was a minimum number of nearby galaxies. These conditions led to a list of FSS plates which were then processed through the normal processing pipe-line. Their average “instrumental” noise is 25 mJy instead of about 40 mJy for more typical FSS plates. Since with these conditions, the reliability of the sample had been verified to be high through spot checks, the extraction thresholds for the normal FSS pipeline (which were set conservatively) were reduced (from S/N of 3 to 2.5) in order to increase the completeness of the VFSS down to 110 mJy at 60 μ m (and similar increases in completeness in the other 3 bands). The resulting VFSS database covers 400 square degrees in 4 separate contiguous regions (Table 1) and contains approximately 2,500 sources detected at 60 μ m. The VFSS is about 2 times deeper than the FSC and contains many unique sources since they can not be found in any other IRAS catalogue or database¹.

Although we have only upper limits at 12, 25 and 100 μ m for the great majority of the 60 μ m detections, a few stars lie

¹ Although the field studied by Hacking & Houck (1987) has one of the highest spacecraft coverages and thus passes condition 2, it fails to pass condition 1 for cirrus contamination and was automatically excluded.

in the sample. We removed them by requesting infrared sources to have $f_{\nu}(25\mu\text{m}) < f_{\nu}(60\mu\text{m})$. This simple criterion proves to filter efficiently most galactic objects, but might also discard a few Seyfert galaxies (e.g. Dennefeld & Veron 1986). However, as only 2% of our detections do not pass the filter criterion (all identified as bright stellar sources in our optical subsample), we consider this effect to be negligible.

3. The “Monte-Carlo” 60 μ m sample

About 2/3 of our detections at 60 μ m have a S/N lower than 5, i.e. a photometric accuracy worse than 20%. At these levels, one expects the data to be seriously affected by completeness and reliability problems. Important photometric errors (if they are not purely fractional) do significantly bias number counts (Eddington 1913), as well as many other statistics that can be drawn from a flux limited survey. Murdoch et al. (1973) have tabulated the Eddington bias, in the typical case of an underlying Euclidean slope and Gaussian flux errors, down to a “safe” 5σ level. For detections lying below this level, the simple analytical correction used by Oliver et al. (1995) from the Murdoch et al. calculations, cannot be applied. The only escape is to proceed through Monte-Carlo simulations. This can be easily done here as both the instrumental and total noise levels are nearly constant over the surveyed zone. We have therefore created mock infrared images mimicking FSS plates, on which was run a source extraction algorithm similar to the original one used for the FSC. Statistics drawn from the simulation catalogs could then be directly compared with those from the real observations, with the hope of discriminating against different models of the IRAS galaxy population.

The Monte-Carlo approach has some limitations at these low S/N levels, mainly because assumptions have to be made about the noise distribution. For this reason, we included only two components in the simulations: “instrumental noise”, which we considered to be Gaussian, and galaxies. Given the very high coverage in our fields, the data conditioning involved in the production of FSS plates (including de-glitching, median filtering and trimmed average) should have removed all significantly non-Gaussian features from the instrumental noise distribution. Filaments from infrared cirrus (Low et al. 1984) are more of a threat, and can easily create false detections by themselves. In what follows, we will keep in mind the possible existence of such noise components. But one can remark that the effect of transient noise sources like cirrus peaks and glitches, whose distributions are strongly skewed toward positive values, is essentially to lower the reliability of detections.

3.1. The galaxy population

We modeled the flux distribution of infrared galaxies assuming a constant comoving number density, and a Saunders et al. (1990) Luminosity Function (LF):

$$\phi(L_{60}) = C \left(\frac{L}{L^*} \right)^{1-\alpha} \exp \left[-\frac{1}{2\sigma^2} \log_{10}^2 \left(1 + \frac{L}{L^*} \right) \right], \quad (1)$$

where $L_{60} = \nu L_\nu$ at $60 \mu\text{m}$, $\alpha = 1.09$, $\sigma = 0.724$ and $L^* = 2.95 \cdot 10^8 h^{-2} L_\odot$. These best-fit parameters depend slightly on the value of H_0 , which was conveniently set to $60 \text{ km.s}^{-1} \cdot \text{Mpc}^{-1}$ in our simulation, close to the value of $66 \text{ km.s}^{-1} \cdot \text{Mpc}^{-1}$ adopted by Saunders et al.. $\phi(L_{60})$ was normalized so as to fit the QDOT galaxy counts (Rowan-Robinson et al. 1991) over the domain $1 < f_\nu(60\mu\text{m}) < 2 \text{ Jy}$. It therefore assumes that evolutionary effects are negligible at this flux level. We adopted the luminosity-dependent fit of Hacking & Houck (1987) to the Soifer et al. (1987) Bright Galaxy Sample, for the distribution of spectral indices. Pure luminosity evolution was introduced in some of the realizations by making the L^* parameter evolve as $(1+z)^Q$. This simple form is not introduced here with strong physical justification, but only to provide a convenient estimator for the evolutionary rate of the galaxy population in the infrared. Luminosity evolution was preferred to density evolution as it is more convenient to simulate through Monte-Carlo methods. At the depth reached by our data, significant evolution can only be probed for FIR-luminous galaxies. As for these galaxies, the LF behaves much like a power-law (Eq. 1), very similar results are obtained for pure density evolution. We gave to the “cool” and “warm” components (Saunders et al. 1990) the same rate of evolution for simplicity. In fact the “warm” (starburst) component proves to be the essential contributor to the part of the LF where evolution can be probed here.

The spatial distribution of galaxies was simulated using a three-dimensional log-normal density field (Coles & Jones 1991), and the Saunders et al. (1992) autocorrelation function truncated at 20 Mpc and kept constant in spatial coordinates. The log-normal model gives a honest fit to the count probabilities in the 1.2 Jy sample (Bouchet et al. 1993) and, although it may be unable to reproduce very high density regions or features like sheets and filaments, it provides an interesting alternative to other simple “toy universe” construction methods (e.g. Soneira & Peebles 1978, Benn & Wall 1995).

The overall simulated galaxy sample was then placed in an Einstein-de Sitter universe, within a rod $150 h^{-1} \text{ Mpc}$ wide, extending up to $z = 2$. This redshift limit was chosen here for practical purpose. It does not affect by more than a few % counts with $f_\nu(60\mu\text{m}) > 10 \text{ mJy}$ for the highest evolution rates considered in this paper. Although (projected) clustering was obvious on simulation images as seen by eye, none of the statistical measurements discussed in this paper proved to be affected significantly if we switched to a simple Poissonian distribution. Nevertheless, all numbers presented here were derived from simulations *with* clustering.

3.2. The images

For the sake of simplicity, we simulated directly IRAS images by projecting galaxies over the frame, without including the complex co-adding of individual scans. The simulated images were given the same pixel size as the original FSS plates: $0.5'$. This generously samples the reconstructed IRAS “point spread function”, thereby removing the need for oversampling

when projecting the infrared sources before convolution. At the same stage, we added white noise to account for instrumental noise. Images were convolved by Fast-Fourier Transform with a $3.7' \times 2.1'$ Gaussian beam (a reasonable fit to the $60 \mu\text{m}$ FSS templates at these ecliptic latitudes), with the minor axis (average “in-scan” direction) aligned with the y-axis. Finally, we suppressed the mean background and low spatial frequencies by applying the standard $60 \mu\text{m}$ zero-sum median filter of the FSS (Moshir et al. 1992) along the y-axis of the image. In the FSS, this point-source filtering was normally done on individual IRAS scans, which implies some angular dispersion in the final images at high ecliptic latitude. Anyway, our simulated “in-scan” point-source profiles are in excellent agreement with those from the original plates.

3.3. Source extraction

The mock catalogue was created from the simulated images by running a slightly modified version of the SExtractor (Bertin & Arnouts 1996) photometry program, tuned to mimic closely the original FSC “Extractor” from IPAC (Moshir et al. 1992). In particular, the standard “clipped rms” estimate of background noise in SExtractor was replaced by the “68%-quantile” from the FSC extractor, and the integrated flux of detected sources by the peak pixel intensity, as for the real data.

4. Infrared statistics

4.1. Confusion noise

It is interesting to compare the average 68%-quantile measured on simulations with those from the real flux-maps (Table 2). This parameter is particularly sensitive to the density of undetected sources: in quadrature, about 2/3 of the confusion noise is expected to come from sources in the 10-100 mJy flux range with the models considered here. The 68%-quantile is fairly stable in our simulations and in the real measurements, and enables us to constrain the number of these faint galaxies. Model-dependent conclusions about the evolution rate can be drawn from it (there is of course a dependence on model normalisation itself, but number counts of bright sources should restrict this uncertainty to less than $\approx 10\%$). As Table 2 shows, the fluctuations predicted by a model evolving as $L^* \propto (1+z)^Q$, with $Q \gtrsim 4$ are too large (the uncertainty quoted here represents the rms of the 68%-quantile over the southern subset area, where it reaches its minimum value). The $Q = 3$ and $Q = 3.5$ models agree well with the data if there is no other contribution than pure instrumental noise affects in our FSS fields. Milder-evolution and no-evolution models may require additional noise, cirrus for example, to fit the data.

Some very faint cirrus can unambiguously be seen in the unfiltered $60 \mu\text{m}$ maps, which means they may somehow contribute to the background confusion noise. Gaultier et al. (1992) have estimated the confusion noise at $60 \mu\text{m}$ due to cirrus to be about 7 mJy rms, at high galactic latitude in the FSC. This might be taken as a typical value for our catalog, as our fields are located at only $|b| \approx 35$, but are amongst the “cleanest” of the

Table 2. 68% quantile statistics in mJy (including 25 mJy *rms* instrumental noise).

VFSS data	no evol. model	$Q = 3$	$Q = 3.5$	$Q = 4$
30.2 ± 1.2^a	28.1	30.1	30.7	32.8

^a standard deviation (see text).

infrared sky concerning cirrus emission, and are comparable to higher galactic latitude zones. Because the infrared surface brightness distribution of cirrus has generally much larger wings than a Gaussian, one should expect their contribution to the total 68%-quantile to be less than 7 mJy in quadrature. However, given the large uncertainties in the real importance of cirrus emission in our fields, we do not discard the possibility of significant cirrus contamination of both background and individual source measurements.

In any case, this fluctuation analysis is consistent with previous estimates that used the integrated infrared background (Oliver et al. 1995), although it is slightly more stringent for the $Q = 4$, $z_f = 2$ model which is only marginally compatible with our data.

4.2. Number counts

Deriving (raw) infrared number counts is straightforward here, as we are dealing with a homogeneous set of data. Comparison with our Monte-Carlo samples is shown in Fig. 1. The Eddington bias is clearly visible below $f_\nu(60\mu\text{m}) \approx 200$ mJy. The best fit value for Q proves to depend on the flux range considered. For $f_\nu(60\mu\text{m}) > 150$ mJy, i.e., for sources above with S/N higher than 5, we find $Q = 3.2 \pm 0.2$, which however raises to $Q = 3.6 \pm 0.3$ if we consider only the 0.15-0.2 Jy range. In the more uncertain 0.11-0.15 Jy domain, we find $Q = 3.9 \pm 0.2$. Accounting for a $\pm 10\%$ possible error in the model normalisation yields a $\approx \pm 0.3$ additional uncertainty to the values of Q quoted above. These numbers may indicate that the $(1+z)^Q$ dependence in luminosity is inappropriate for describing the effect seen here. However, we shall remember that, as stressed earlier, assumptions about the noise distribution become very critical in the 0.11-0.15 Jy bin and will affect conclusions made with low S/N data.

This brings the question of whether our fields represent a “fair sample” of the Universe, i.e. is there a relative excess of faint or bright sources due to large scale-structures which could distort the statistics (see e.g. Lonsdale & Hacking 1990)? Fortunately this point can be addressed using our bright optical galaxy counts in the same areas (paper I). Expressed with the same magnitude scale, they are similar to those done on much larger catalogs (APM, COSMOS) in the $17 < B_J < 21$ range, where most of the optical counterparts to faint IRAS sources lie. A strong distortion of galaxy counts induced by the presence of large scale structures is thus excluded.

An interesting question is: what happens to number counts if we add some Gaussian noise to the no-evolution model, in order to reach the observed intensity of fluctuations? The answer is: almost nothing, as can be seen in Fig. 1. As expected, this test

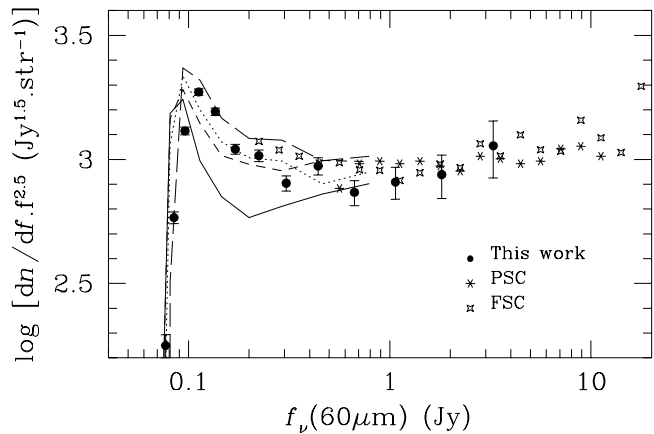


Fig. 1. Raw number counts compared with models at $60 \mu\text{m}$. The PSC/QDOT (Rowan-Robinson et al. 1991) and FSC (Lonsdale et al. 1990) counts have been added for comparison. The FSC counts are not corrected for the Eddington bias, and so their two faintest bins are probably overestimated. For clarity, the Monte-Carlo models were plotted only for fluxes below 1 Jy. *solid*: no-evolution + Gaussian noise (see text); *dashes*: evolution with $Q = 3$; *dots*: $Q = 3.5$; *long dashes*: $Q = 4$. Error bars are Poissonian uncertainties. Monte-Carlo models become very noisy brightward of 1 Jy, and have not been drawn there for clarity. Note that the bin size is not constant.

indicates that the no-evolution model could be saved only if the distribution of “hidden” noise components is extremely non-Gaussian, creating noise peaks without increasing too much the 68% quantile.

5. Optical identifications

In order to find out whether the faint source excess measured in the previous sections is real or contaminated by noise peaks, some identification work is necessary. Systematic studies conducted at higher IRAS flux limits (e.g. Wolstencroft et al. 1986, 1992, Sutherland & Saunders 1992) have shown that the optical domain is well adapted to this task.

5.1. The data

Thirty percent (6 Schmidt plates) of the VFSS were analysed using photographic data in the blue B_J and red R_F passbands. The sensitivity of deep survey plates is well matched to our IRAS study, as the VFSS error box at the faintest flux levels occupies roughly 1 square-arcminute on the sky, and contains already an average of ≈ 0.3 galaxies brighter than $B_J = 21$. Full details about the optical catalog can be found in Paper I; we summarize here its main features. This catalogue is quite small compared to large galaxy surveys like APM (e.g. Maddox et al. 1990) or COSMOS (e.g. Heydon-Dumbleton et al. 1989), but is well calibrated (within ≈ 0.1 mag, thanks to a high density of photometric standards). The completeness for galaxies is expected to be better than a conservative 90% at least for $17 \leq B_J \leq 20$. Brighter than this, there might be some loss

due to inaccurate star-galaxy separation, and underestimation of fluxes (≈ 0.1 mag) because of photographic saturation effects. Positions are accurate within a fraction of arc-second. This is sufficient for identifying faint IRAS sources, which have typical positional uncertainties of a fraction of arcminute.

5.2. The simulated optical sample

As for the infrared statistics presented in the previous sections, extreme caution should be taken in interpreting the results of optical identifications. We don't know a priori what fraction of *real* IRAS sources can be identified, especially given the large errors in $f_\nu(60\mu\text{m})$ at our flux level. Here again, we addressed this question using a Monte-Carlo method, by simulating a sample of identified optical counterparts to the artificial sample described in Sect. 3.

5.2.1. Optical luminosity

We first assigned some random optical luminosity to each infrared ‘‘Monte-Carlo’’ galaxy with theoretical flux received on Earth $f_\nu(60\mu\text{m}) > 10$ mJy, according to a suitable optical/ $60\mu\text{m}$ distribution. This is an easier task than it may appear, as IRAS and bright optical galaxy catalogs do have an overlap large enough so that one can build a local, bivariate luminosity function. The most comprehensive study in that field was done by Saunders et al. (1990), who proposed a Gaussian distribution of the blue absolute luminosity, with standard deviation $\sigma_M = 0.72$ and mean

$$\mu_M = -19.9 + 5 \log h + 0.3 \left(\log \frac{L_{60}}{L_\odot} - 11.24 - \log h^{-2} \right)^2. \quad (2)$$

Note that the original expression contains a sign error. M normally refers here to a B_T^0 magnitude, which corresponds almost to our B_J magnitude system (Paper I) as we drop the average correction for internal extinction $A_i = 0.21$ (Rowan-Robinson 1987). Although (2) is based on limited statistics and rather inaccurate optical magnitudes, we believe it does provide a globally correct description of the link between the $60\mu\text{m}$ and blue luminosity functions because: 1) relation (2) correctly reproduces both the L_{FIR}/L_B distribution for ‘‘normal’’ luminosity sources (Rowan-Robinson et al. 1987, Bothun et al. 1989) and the ‘‘saturation’’ of optical luminosities observed in Ultraluminous InfraRed Galaxies (ULIRGs) (Smith et al. 1987, Soifer et al. 1987); 2) integrating over all possible infrared luminosities leads to a blue luminosity function in excellent agreement with recent, local determinations² (e.g. Ellis et al. 1996). The bivariate luminosity function based on (1) and (2) is shown in Fig. 2. We assume relation (2) to hold out to $z \approx 0.3$, corresponding to the most distant, luminous galaxies we might detect in numbers both in FIR and in the optical. This obviously supposes a negligible evolution of their dust content over the corresponding period of time. We shall tackle this point in Sect. 7.

² It is interesting to note that this leads to a ‘‘high’’ normalisation of the *local* blue luminosity function, in agreement with our bright optical counts (Paper I).

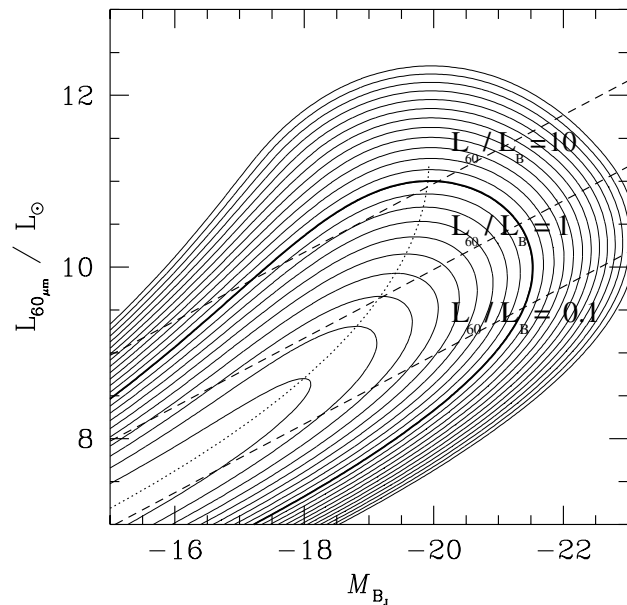


Fig. 2. Contour plot of the assumed bivariate $60\mu\text{m}/B_J$ galaxy luminosity function, from the parameterization work of Saunders et al. (1990). There is a factor 2 in density from one contour to another. The luminosity range analysed by Saunders et al. is approximately delineated by the heavier contour. The dotted curve represents Eq. (2). Dashes indicate lines of constant L_{60}/L_B .

5.2.2. k -corrections

In order to give the right optical k -corrections to our simulated IRAS sources, one has to make some general assumption about their optical/UV spectral energy distribution (SED). The large majority of IRAS galaxies contained in FIR flux-limited samples are spirals (e.g. de Jong et al. 1984), with average morphological type Sbc (Bothun et al. 1989, Sauvage & Thuan 1994). Although their rest-frame optical colours span a considerable range, it is difficult to find an obvious trend with FIR luminosity (Leech et al. 1988, 1989, Hutchings & Neff 1991). An Sbc SED also proves to reproduce satisfactorily the observed optical continuum of 1.4-GHz sub-mJy starburst galaxies with $B < 22$ (Benn et al. 1993). Given the tight correlation existing between radio-continuum and far-infrared galaxy luminosities (de Jong et al. 1985, Helou et al. 1985), $f_\nu(1.4\text{GHz}) \approx 10^{-2} f_\nu(60\mu\text{m})$, these sources are representative of the faintest ones we might detect in our $60\mu\text{m}$ sample. We have therefore adopted the Sbc SED from Pence (1976) to compute optical k -corrections through our B_J and R_F pass-bands, and the average Sbc $\langle B_J - R_F \rangle = 0.96$ typical rest-frame colour from Paper I. We will find in Sect. 5.5 other arguments justifying this choice.

We finally end up with a large number of artificial sources having in addition to their ‘‘unbiased’’ $f_\nu(60\mu\text{m})$ fluxes, B_J and R_F magnitudes that could directly go through the same complex IR detection and optical identification processes, as real galaxies.

5.3. Identification method

Because of the low resolution of IRAS images ($\approx 2'$ at $60 \mu\text{m}$), the reliability of the identification technique is crucial for finding the right optical counterparts to faint infrared sources. This is even more critical here, because of the particularly low infrared S/N and optical faintness for most of the candidates. We have adopted the likelihood-ratio method, inherited from radio-source identification programs (de Ruiter et al. 1977, Prestage & Peacock 1983), which was successfully applied in previous IRAS studies (Wolstencroft et al. 1986,1992, Sutherland & Saunders 1992).

The positional uncertainty of an IRAS detection is essentially a function of the local reconstructed IRAS point spread function and the S/N. Assuming the error distribution is roughly Gaussian, this defines the traditional error ellipses around the estimated object position, described by the σ_x , σ_y and θ ; respectively the *rms* error along the major axis (cross-scan), the *rms* error along the minor axis (in-scan), and position angle. Switching to the reduced coordinate:

$$r = \sqrt{\frac{X^2}{\sigma_X^2} + \frac{Y^2}{\sigma_Y^2}}, \quad (3)$$

we can express the probability for the true optical counterpart to lie between r and $r + dr$ as

$$p_r(r) dr = Q e^{-r^2/2} r dr \quad (4)$$

where Q is the probability for the infrared detection to exist and to be detectable in the optical catalogue. In order to check that this modeling fits the data correctly, we derived maximum-likelihood estimates of σ_x , σ_y and θ from optical identifications of the brightest infrared sources ($f_\nu(60 \mu\text{m}) > 0.2 \text{ Jy}$). We were able to recover the catalogue values within 10-20%. Of course, this does not mean that the modeling is *adequate*. There is indeed some evidence that the wings of the positional error distribution are larger than Gaussian ones (e.g. Sutherland & Saunders 1992); we will quantify the consequences of this effect in the next section. As shown in Fig. 3, the Gaussian model proves to fit correctly the distribution of optically bright ($B_J < 17$) counterparts in our catalogue. One can however already detect a slight excess ($\approx 5\%$ of the total) of identifications at about 3σ along the cross-scan direction.

Equation (4) defines the probability density for a genuine identification to lie around the IRAS detection. We can compare it to the probability of encountering by chance an optical object of class c , brighter than magnitude m between r and $r + dr$:

$$p_f(r, m, c) dr = 2\pi\sigma_X\sigma_Y N_c(m) r dr, \quad (5)$$

where $N_c(m)$ is the projected density of optical objects with class c brighter than m . This leads to the likelihood ratio definition from Wolstencroft et al. (1986):

$$L(r, m, c) = \frac{p_r(r, m, c)}{p_f(r, m, c)} = \frac{Q e^{-r^2/2}}{2\pi\sigma_X\sigma_Y N_c(m)}. \quad (6)$$

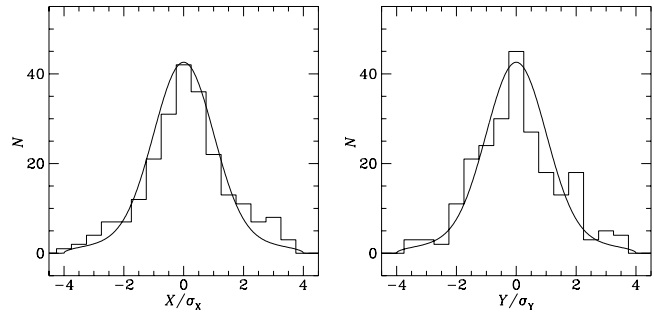


Fig. 3. Distribution of the 227 galaxies with $B_J < 17$ and $r \leq 4$ detected around infrared sources, along the major (left) and minor axes of the IRAS error ellipse (histogram). When several galaxies pass this criterion, the barycenter of the group is taken. The model (curve) assumes Gaussian positional errors and take into account contamination by “chance” counterparts ($\approx 6\%$ at center of ellipse).

Sutherland & Saunders (1992) stressed that L is independent of the number of optical candidates lying in the error ellipse. Some extra information can be gained from the presence or absence of these other candidates if one assumes that the true optical counterpart to the infrared source is unique. However, this hypothesis is dangerous for IRAS galaxies, because of the non-negligible fraction of multiple systems optically identified (e.g. Gallimore & Keel 1993). Besides, the artificial and real optical galaxy samples do not have the same density of “background” galaxies, as the first one comes from an infrared flux-limited sample: any estimator that combines information from the other optical detections is likely to behave differently in both cases. We therefore conformed to the “standard” likelihood ratio L as an *individual* identification estimator for optical candidates.

For every IRAS detection lying within the area of our optical catalog, likelihood ratios L_i associated to every potential optical candidate were obtained in the following way. First, we estimated the $N_c(B_J)$ separately for stars ($c = S$) and galaxies ($c = G$) from the number counts relative to the current plate. Then we defined a circular zone with a $3'$ radius around each IRAS position. This corresponds to a large confidence interval for r : at least 6σ , or a diameter 3 times larger than the IRAS beam FWHM. Finally, the L_i were computed using (6) for all optical detections within the circular zone. The same procedure was applied to the artificial optical sample around detections in the simulated $60 \mu\text{m}$ images, but this time using $N_G(m) = \text{dexp} 0.5(B_J - 15.0)$, which provides a good fit to our integrated galaxy number counts per square degree (paper I). The sizes of the “artificial” error ellipses were computed with formulae (II.F.5) and (II.F.6) in Moshir et al. (1992), assuming the number of scans to be $\langle N \rangle = 20$, and a background noise of 30.2 mJy .

5.4. Identification rate

What *real* fraction of infrared sources possess one or more optical counterparts? Using the individual likelihood ratios L_i , we can define a global estimator \mathcal{L} for each IRAS detection, from

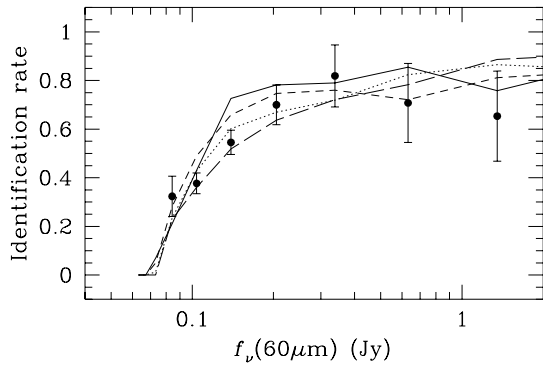


Fig. 4. Identification rate (corrected for the effects of spurious identifications) of IRAS sources with a likelihood threshold of 5. The lines are the Monte-Carlo models, as in Fig. 1.

which we will derive an identification ratio. Here again, we need to be able to compare statistics done with different densities of contaminating sources. For this reasons, we have chosen

$$\mathcal{L} \equiv \sup(L_i), \quad (7)$$

though it might certainly be less effective for multiple sources than, e.g. $\mathcal{L} \equiv \sum_i L_i$. In the presence of contamination by “chance” optical objects, the observed probability for \mathcal{L} [as defined by (7)] to exceed some threshold \mathcal{L}_0 for an infrared detection reads:

$$p(\mathcal{L} > \mathcal{L}_0) = p_r(\mathcal{L} > \mathcal{L}_0) (1 - p_f(\mathcal{L} > \mathcal{L}_0)) + p_f(\mathcal{L} > \mathcal{L}_0), \quad (8)$$

where $p_r(\mathcal{L} > \mathcal{L}_0)$ and $p_f(\mathcal{L} > \mathcal{L}_0)$ are the probabilities to have $\mathcal{L} > \mathcal{L}_0$ because of real and fortuitous optical identifications, respectively. Thus

$$p_r = \frac{p - p_f}{1 - p_f}. \quad (9)$$

p_f can be measured by putting error ellipses at random positions in both real and artificial catalogs, which then enables us to compare the real identification rates p_r .

Figure 4 shows p_r as a function of the 60 μm flux, for $\mathcal{L}_0 = 5$ (which proves to be a good compromise between completeness and reliability). Although they do not enable us to choose between the models, these statistics seem to indicate that the faintest infrared sources cannot be attributed to a large number of unexpected “noise peaks”. Another interesting result is the rather low identification rate predicted by simulations at high S/N: about 80%. This in good agreement with the observations, and the $\approx 90\%$ identification rates reported for the FSC (Sutherland et al. 1991, Wolstencroft et al. 1992), once the differences in the sizes of error ellipses and the addition of chance identifications have been accounted for. An examination of the simulated FSS images reveals that the unidentified sources are produced by confusion with close neighbours in projection. Because of the large width of the IRAS beam, the barycenter of

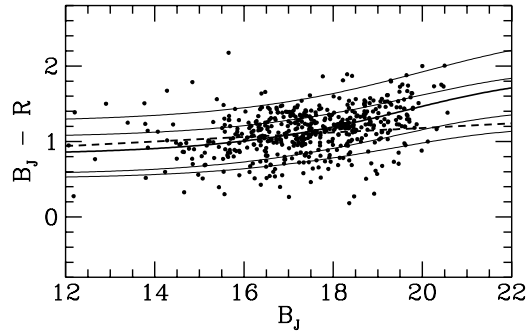


Fig. 5. Colour-magnitude diagram of all optical counterparts to IRAS sources with $\mathcal{L} > 10$, in the photographic B_J and R bands (points). This high threshold in likelihood limits the proportion of fortuitous sources to about 10%. Solid curves are the average colour tracks predicted by the non-evolving model described in the text, assuming different k -corrections. From top to bottom: E/S0, Sab, Sbc (*heavy line*), Scd and Sdm. For comparison, the dashed line indicates the average colour of our complete optical galaxy sample as a function of magnitude.

some detections can be shifted by a few pixels, i.e. 5σ or more at high S/N, adding a long tail to the Gaussian error distribution. For these detections, the measured likelihood ratio of the optical counterpart(s) is thus very close to zero. We conclude that this phenomenon might be responsible most of the high S/N unidentified point-sources in the FSC. Note that cirrus sources do also constitute potential deflection factors.

5.5. Optical colour distribution

The colour distribution for all identifications with $\mathcal{L} > 10$ (roughly a 10% contamination) is shown in Fig. 5, together with the average colour tracks produced by the differential k -corrections computed with the Pence (1976) SEDs. For clarity, only the no-evolution model is plotted. The $Q = 3, 4$ models yield tracks very similar to those of the no-evolution model, which is normal as Eq. (2) provides very little evolution in optical luminosity for luminous FIR sources. The dispersion in colours appears to be substantially smaller than for an optically limited sample, and as can be seen, the bulk of the IRAS population follows quite closely the Sbc type, supporting our choice in Sect. 5.2.2 to adopt an Sbc type for the average optical k -correction.

5.6. Magnitude distribution

We now turn to comparing the magnitude distribution with model predictions. Once again, we have to subtract the contribution from fortuitous detections. One can decompose the total observed number of identifications per magnitude bin at magnitude m , $n(m)$, as

$$n(m) = (1 - p_f)n_r(m) + (1 - p_r)n_f(m) + n_c(m), \quad (10)$$

where $n_r(m)$ is the number of real counterparts and $n_f(m)$ the number of fortuitous optical galaxies in the same magnitude

interval. $n_c(m)$ represents the contribution from IRAS sources for which both real and fortuitous identifications can occur (with probability $p_r p_f$). We don't know $n_c(m)$, but we can safely bracket it between the two extreme cases:

$$0 \leq n_c(m) \leq p_f n_r(m) + p_r n_f(m). \quad (11)$$

The lower bound corresponds to the case where the magnitude bin is totally depleted by the presence of the two ‘‘competitors’’, and the higher bound corresponds to the case where there is no depletion at all. The true value is quite probably intermediate. Inserting $n_c(m)$ in (10) we get

$$n(m) - n_f(m) \leq n_r(m) \leq \frac{n(m) - \left(\frac{1-p}{1-p_f}\right) n_f}{1-p_f}. \quad (12)$$

The magnitude distribution of IRAS sources with $\mathcal{L} > 5$ is plotted in Fig. 6, together with model predictions, for two $60 \mu\text{m}$ flux domains. As expected from the evolution models, excess sources are found on the dim side of the histogram. A very good agreement is found for $3 < Q < 4$, but like the identification rate statistics, they do not put further constraints to the exact amount of evolution.

6. Summary and comparison with other works

Although they cannot be considered as really independent one from each other, the results of the four statistical tests described above (background fluctuations, number counts, identification rate and magnitude distribution) do provide a picture remarkably consistent with the phenomenological $L^* \propto (1+z)^Q$ evolution model, with $3 < Q < 4$. The most stringent test is given by the number counts with $Q = 3.2 \pm 0.2 \pm 0.3$ down to 0.15 Jy , with some indication of a stronger evolution below 0.2 Jy . However, the fluctuation analysis indicates that Q cannot increase much beyond $Q = 4$ below 0.1 Jy . As indicated earlier, a pure density evolution yields a similarly good fit to the data, with a comoving density evolving as $\propto (1+z)^{6.0 \pm 0.5 \pm 0.7}$ down to 0.15 Jy .

These values are in good agreement with the value found on shallower surveys by Saunders et al. (1990) who found $Q = 3.1 \pm 1.0$ —although according to some authors, e.g. Fisher et al. 1992 or Oliver et al. 1995, this number might largely be affected by biases —, and Oliver et al. (1995) with $Q = 3.3 \pm 0.8$. However they do *a priori* rule out the extreme evolution discovered by Gregorich et al. (1995) in their IRAS number counts. In particular, their high density of faint sources is incompatible with our background fluctuation analysis. A check done on the Gregorich et al. (1995) fields reveals that they contain cirrus, which might produce a large fraction of false detections, and should also contribute significantly to the total background noise and its associated Eddington bias. Strong cirrus emission also affects the Hacking & Houck (1987) deep field, but the dispersion in their scanning angles smoothes considerably edge-effects on cirrus structures. This might explain why their counts are in better agreement with ours. Our counts and those from previous studies are summarized in Fig. 7.

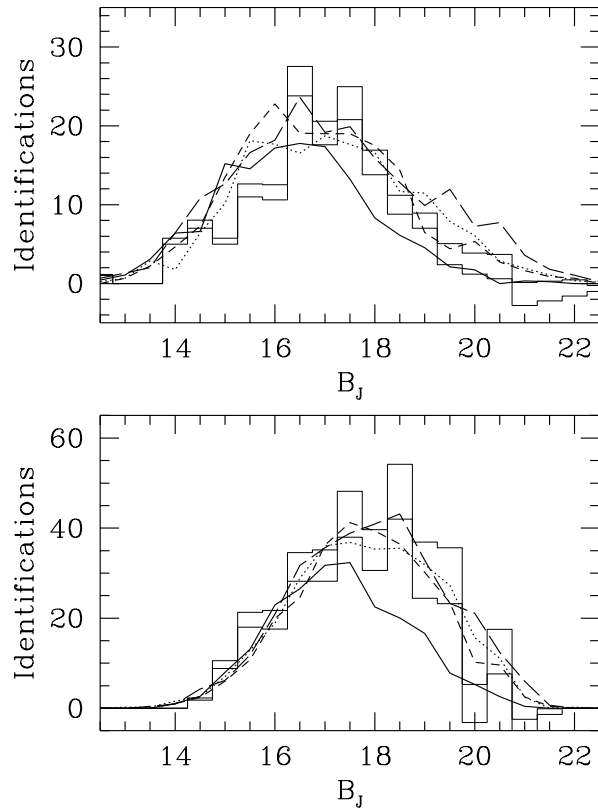


Fig. 6. Magnitude distribution of the optical counterparts to IRAS sources in the photographic B_J band in two infrared flux domains. Up: $0.2 < f_\nu(60\mu\text{m}) < 1 \text{ Jy}$, down: $0.11 < f_\nu(60\mu\text{m}) < 0.2 \text{ Jy}$. The two histograms are the lower and higher limits to the observations induced by the correction of spurious identifications (see text), but do not include Poissonian uncertainties. The lines are the models as in Fig. 1. Note that the optical catalogue is expected to become incomplete for $B_J > 20$ and $B_J \leq 16$.

7. Discussion

7.1. The nature of the faint source excess

Our statistics probes mainly the evolution of infrared luminous galaxies ($L_{60} > L^*$). The good fits given to the data by the $L^* \propto (1+z)^{3.2}$ model, and the large excess of faint optical counterparts indicate that luminous IRAS galaxies should be ≈ 5 -7 times more numerous at $z \approx 0.3$ than at the present time. What are these galaxies? According to our Monte-Carlo model, the optical counterparts with $20 < B_J < 21$ should have an average $60 \mu\text{m}$ luminosity $L_{60} \approx 5.10^{11} h^{-2} L_\odot$ and should be at a redshift $z \approx 0.3$, in agreement with their rather red colours $B_J - R_F \approx 1.6$, if their optical continuum is close to that of local Sbc's. These are therefore potential UltraLuminous InfraRed (ULIRGs) candidates. This picture is consistent with the redshift distribution of the optically faint ULIRGs surveyed by Clements et al. (1996a). Objects with brighter optical counterparts ($B_J < 20$) have naturally a lower FIR excess, but most are still *redder* than the average population in the same magnitude domain. They are very probably similar to the population

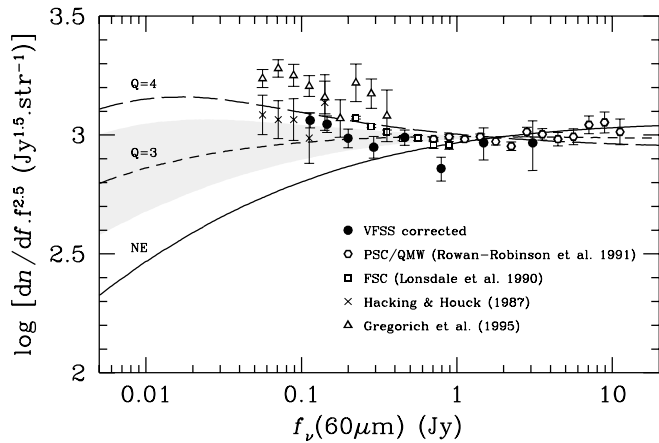


Fig. 7. Corrected VFSS number counts compared with previous studies and simple no-evolution (NE) and $L^* \propto (1+z)^Q$ models at $60 \mu\text{m}$. The correction was done by subtracting to each bin ($f_\nu(60 \mu\text{m}) < 0.3 \text{ Jy}$) the bias measured in Monte-Carlo simulations, with the $Q = 3.5$ model. This bias depends weakly on the exact value of Q ; for $3 \leq Q \leq 4$, the typical uncertainty is $\approx 5\%$, and has been included in the error bars. Note that the other counts have not been corrected for the Eddington bias, and might be overestimated in their faintest bins. The grey area indicates approximately the 1σ confidence domain for number counts in the context of a $L^* \propto (1+z)^Q$ pure luminosity evolution model, drawn from the background fluctuation analysis (Sect. 4.1).

of starburst spirals with $\approx M^*$ optical luminosities identified in the sub-millijansky radio surveys³ (Benn et al. 1993, Windhorst et al. 1995), although at smaller redshifts ($z \approx 0.1-0.2$). Hence it seems unlikely that a large fraction of the detected excess of faint $60 \mu\text{m}$ sources at the 100 mJy level might be caused by dust-enriched primeval galaxies, as suggested by Franceschini et al. (1994).

Wang (1991a, 1991b) proposed a pure FIR-luminosity evolution scenario based on the evolution of dust content in normal galaxies. Although some variants of this model might be able to predict a significant increase of FIR luminosity in galaxies over the few past Gyr, they rely on the assumption that emitters are optically thin at blue/UV wavelengths. This is certainly not the case for most of FIR-luminous galaxies (the sole population of galaxies that can be detected by IRAS at significant redshifts). As these objects already have $L_{\text{FIR}} > L_{\text{B}}$, adding more dust should not be very effective in increasing their FIR luminosities (e.g. Belfort et al. 1987). Therefore a moderate change in the dust content of galaxies since $z \approx 0.3$ should not be a major contributor to the evolution observed yet for IRAS galaxies.

The evolution rate of luminous IRAS galaxies is in remarkable agreement with those of QSOs (e.g. Boyle et al. 1988) or X-ray selected Active Galactic Nuclei (AGN) (e.g. Maccacaro et al. 1991), which brings up the link between AGN and ULIRGs, as most of the latter may harbour AGNs (e.g. Sanders et al. 1988). An important question is therefore: does the evolution concern the global FIR-luminous galaxy population, or

is it limited to “monsters” containing active nuclei? The magnitude distribution in our faintest $60 \mu\text{m}$ flux bin (Fig. 6) seems to indicate that most of the sources found in excess are not ULIRGs, and consequently, according to local statistics (Leech et al. 1989), are less likely to contain an AGN. A stronger argument against a sample dominated by AGNs may come from spectroscopic identifications of sub-millijansky radio-sources (Benn et al. 1993), which, as we saw, can be compared to our sample, and has proven to contain a minority of AGN-like spectra. Extreme caution should however be made in interpreting these spectra, as optical signatures of a central engine might be hidden by the large amounts of dust present in the nuclear regions of such objects (see e.g. Dennefeld 1996).

7.2. The link with optical evolution

Deep number counts conducted at visible wavelengths have revealed a large excess of faint galaxies over the no-evolution predictions from $q_0 > 0$ cosmological models (Tyson 1988, Colless et al. 1990, Lilly et al. 1991, Metcalfe et al. 1991, 1995, Smail et al. 1995), as well as a blueing of the global population with fainter magnitudes. The $z < 1$ redshift distributions obtained from spectroscopic surveys are however apparently in good agreement with no-evolution models, which suggests a diminution or a fading with time of low and moderate luminosity members of the blue galaxy population⁴ since $z \approx 0.5$ (Broadhurst et al. 1988, Lilly 1993, Ellis et al. 1996, Driver et al. 1995). Various scenarios to explain this observational phenomenon have been proposed, including a delayed formation epoch of dwarf galaxies (Babul & Rees 1992, Babul & Ferguson 1996), decimation through intense merging (Guideroni & Rocca-Volmerange 1991, Broadhurst et al. 1992), or more prosaically, biases in the determination of the local luminosity function (Davies 1990, McGaugh 1994, Gronwall & Koo 1995).

Now, strong evolution among the spiral population, apparently seen at FIR and radio wavelengths, is a tempting argument for hypotheses advocating recent evolution of the optical LF. Evolution in FIR is detected in redshift surveys of IRAS samples (Saunders et al. 1990, Oliver et al. 1995) and could be explained, for example, through an increasing rate with z of galaxy-galaxy interactions, which are known to be efficient triggers of starburst activity (e.g. Larson & Tinsley 1978), or AGNs (Sanders et al. 1988). There are indeed both theoretical (Toomre 1977, Carlberg 1990) and observational (Zepf & Koo 1989, Burkey et al. 1994, Carlberg et al. 1994) evidences for such a rapid increase with redshift of the merging rate, at least to $z \approx 0.7$. A few attempts have been made to link a strong, starburst-driven, evolution of the FIR luminosity function to that of the optical (Lonsdale & Harmon 1991, Lonsdale & Chokshi 1993, Pearson & Rowan-Robinson 1996). They involved simple proportionality between the optical and FIR evolution (either in density or luminosity) and therefore predicted a large increase in the comoving space density of optically bright

³ Incidentally, the evolution of sub-mJy radio sources seems compatible with that of IRAS galaxies (Rowan-Robinson et al. 1993).

⁴ For simplicity, we shall refer to these objects as “faint blue galaxies”.

($M < M^*$) galaxies with redshift, which is unfortunately not seen at $z < 0.5$. The same problem arises with stellar population synthesis models applied to starburst-driven evolution (e.g. Carlberg & Charlot 1992, McLeod & Rieke 1995).

But this apparent contradiction could be alleviated by remarking that the possibly large increase of blue continuum emission resulting from starburst activity is often largely *hidden* at blue/UV wavelengths in FIR luminous galaxies. It is a fact that the complex role of dust, and in particular its geometry with respect to the stars, has been ignored in many models trying to reproduce number counts with starburst-evolution. In massive spirals, star-formation induced by merging is generally concentrated in the central regions of the galaxy (e.g. Hummel 1981, Condon et al. 1982, Bushouse 1987). Such a feature is likely to originate from radial inflow of disk gas triggered by the interaction, and is well reproduced in numerical simulations (e.g. Hernquist 1989, Minhos & Hernquist 1994). The associated circumnuclear starburst (which may surround an AGN) is usually heavily reddened in the optical, and does not increase so much the total blue/UV light output of the galaxy: ULIRGs are rarely “ultraluminous” at visible wavelengths (as reflected by relation 2). On the contrary, starbursts in field dwarf galaxies, dominated by gas-rich, dust-deficient late types (e.g. Van den Bergh & Pierce 1991, Wang & Heckman 1996) typically show up in optically prominent giant H II regions (e.g. Huchra 1987), and are often found to dominate the total blue/UV emission. Hence, statistically, starbursts observed in both types of galaxies possess very different observable signatures. Therefore the hypothesis that starburst galaxies which dominate IRAS faint number counts are the same as those that make the excess seen in the optical at intermediate redshifts (Pearson & Rowan-Robinson 1996) is not convincing.

There is nevertheless evidence from optical redshift surveys that the galaxies with $M \geq M^*$ observed in excess at $z \lesssim 0.5$ are actively star-forming galaxies (Ellis 1996, and references therein). Recent studies have estimated their evolution in terms of global brightening at blue wavelengths between now and $z \approx 0.3 - 5$ to $\approx 1 - 1.5$ mag (Driver et al. 1996, Rix et al. 1996), similar to what we inferred for IRAS galaxies in FIR. Is the evolution of FIR-luminous galaxies closely related to that of faint blue galaxies? In the hypothesis of a recent evolution dominated by starburst processes in both populations, this question is essentially linked to the existence of a common triggering mechanism, in which case we may consider IRAS galaxies as massive, dusty versions of the faint blue galaxies. Although interaction/merging seems to be the rule among distant IRAS galaxies, at least for the most luminous members (Clements et al. 1996b, 1996c), the situation is much less clear for faint blue galaxies. Deep *Hubble Space Telescope* images present visual evidence for a high proportion of interacting/merging objects, increasing steeply with magnitude (Driver et al. 1995, van den Bergh et al. 1996). Nevertheless, many of these sources may well be luminous galaxies at much higher redshifts, or in some cases, knots of star-formation observed in single objects. Besides, optical observations of nearby dwarf galaxies undergoing starbursts reveal that a large fraction are apparently isolated

objects (Campos-Aguilar & Moles 1991, Telles & Terlevich 1995), which argues against interactions as a unique triggering mechanism of starburst activity at recent epochs. Still, one cannot exclude the hypothesis of interactions or collisions with HI clouds, supported by 21 cm observations of the environment of nearby HII galaxies (Taylor et al. 1995).

Another test of the interaction scenario might be provided by studying the spatial (or angular) two-point correlation function. One could expect the distribution of sources triggered by interactions to exhibit some differences with respect to the global (late-type) density field. In fact both IRAS and blue galaxies happen to have clustering properties barely distinguishable, within measurement errors, from their common parent population of late-type galaxies (e.g. Infante & Pritchet 1995, Mann et al. 1996, Oliver et al. 1996), although this may not be true at very small scales (Carlberg et al. 1994, Infante et al. 1996).

We shall therefore conclude this discussion by pointing out that a simple and appealing scenario, in which the strong, recent evolution among late-type galaxies at moderate redshifts is related to an increase of the merging/interaction rate with lookback time, appears qualitatively compatible with the observations. In this scenario, FIR-luminous galaxies would then represent the massive, dusty counterparts of faint starbursting blue galaxies. More data are clearly necessary to test this hypothesis on the observational side, under others to follow the evolution of the intermediate luminosity population in the FIR. This should be possible with the ISO (*Infrared Space Observatory*) satellite. It would also allow to assess more accurately the evidence for strong evolution at low redshifts in the FIR, deduced so far only from IRAS measurements.

8. Conclusions

We have analysed a deep homogeneous 60 μm subsample of galaxies, at the lowest flux limit reached by the IRAS Faint Source Survey, yielding the following results:

1. Detection and measurement biases were assessed through Monte-Carlo simulations, which prove to reproduce satisfactorily most observed features of detected IRAS sources at 60 μm . In particular, the rather high proportion of unidentified sources in the FSC ($\geq 10\%$) can totally be accounted for by deflections caused by neighbouring IR sources.

2. Background fluctuation analysis and number counts provide evidence for strong evolution in FIR luminosity $\propto (1+z)^{3.2 \pm 0.2 \pm 0.3}$ or density $\propto (1+z)^{6.0 \pm 0.5 \pm 0.7}$, in agreement with previous studies.

3. Sources in excess are genuine and are generally associated with faint, relatively red, optical counterparts which we interpret as being M^* massive starbursting galaxies at redshifts $\gtrsim 0.1$.

4. Photometric properties of distant IRAS galaxies suggest that the advocated starbursts (or AGNs) are considerably hidden by dust at UV/visible wavelengths, which would explain why no large number of related optically luminous objects is showing up in optical surveys at $z \leq 0.5$.

5. Faint IRAS galaxies in excess are unlikely to be the ones making the excess in number counts at blue wavelengths and

$z \leq 0.5$, but this does not exclude that both populations follow the same evolution mechanism (i.e. interaction-induced starbursts).

Acknowledgements. The authors wish to thank A. Fruscione for her contribution during an earlier phase of the project, and C. Lidman for helpful comments on the manuscript. One of us (EB) acknowledges an ESO studentship while part of this work was completed.

References

- Babul A., Rees M.J., 1992, MNRAS 255, 346
 Babul A., Ferguson H.C., 1996, ApJ 458, 100
 Belfort P., Mochkovitch R., Dennefeld M., 1987, A&A 176, 1
 Benn C.R., Rowan-Robinson M., McMahon R.G., Broadhurst T.J., Lawrence A., 1993, MNRAS 263, 98
 Benn C.R., Wall J.V., 1995, MNRAS 272, 678
 Bertin E., Arnouts S., 1996, A&AS 117, 393
 Bertin E., Dennefeld M., 1996, A&A 317, 43
 Bothun G.D., Lonsdale C.J., Rice W., 1989, ApJ 341, 129
 Bouchet F.R., Strauss M.A., Davis M. et al., 1993, ApJ 417, 36
 Boyle B.J., Shanks T., Peterson B.A., 1988, MNRAS 235, 935
 Broadhurst T.J., Ellis R.S., Shanks T., 1988, MNRAS 235, 827
 Broadhurst T.J., Ellis R.S., Glazebrook K., 1992, Nature 355, 55
 Burkey J.M., Keel W.C., Windhorst R.A., Franklin B.E., 1994, ApJ 429, L13
 Bushouse H.A., 1987, ApJ 320, 49
 Campos-Aguilar A., Moles M., 1991, A&A 241, 358
 Carlberg R.G., 1990, ApJ 350, 505
 Carlberg R.G., Charlot S., 1992, ApJ 397, 5
 Carlberg R.G., Pritchett C.J., Infante L., 1994, ApJ 435, 540
 Clements D.L., Sutherland W.J., Saunders W. et al., 1995, MNRAS 279, 459
 Clements D.L., Sutherland W.J., McMahon R.G., Saunders W., 1996, MNRAS 279, 477
 Clements D.L., Baker, A.C., 1996, A&A 314, L5
 Cole S., Ellis R.S., Broadhurst T.J., Colless M.M., 1994, MNRAS 267, 541
 Coles P., Jones B., 1991, MNRAS 248, 1
 Colless M.M., Ellis R.S., Taylor K., Hook R.H., 1990, MNRAS 244, 408
 Condon J.J., Condon M.A., Gisler G., Puschell J.J., 1982, ApJ 252, 102
 Davies J.J., 1990, MNRAS 244, 8
 de Jong T. et al. , 1984, ApJ 278, L67
 de Jong T., Klein U., Wielebinski R., Wunderlich E., 1985, A&A 147, L6
 Dennefeld M., Véron-Cetty M.P., 1986, in Light on Dark Matter (ed. F.P. Israel), Reidel, Dordrecht, 493
 Dennefeld M., 1996, IAU colloquium 159, in press
 Driver S.P., Windhorst R.A., Ostrand E.J., Keel W.C., Griffiths R.E., Ratnatunga K.U., 1995, ApJ 453, 48
 Driver S.P., Couch W.J., Phillipps S., Windhorst R.A., 1996, ApJ 466, L5
 Eddington A.S., 1913, MNRAS 73, 359
 Ellis R.S., Colless M., Broadhurst T., Heyl J., Glazebrook K., 1996, MNRAS 280, 235
 Fisher K.B., Strauss M.A., Davis M., Yahil A., Huchra J.P., 1992, ApJ 389, 188
 Franceschini A., Danese L., De Zotti G., Xu C., 1988, MNRAS 233, 175
 Franceschini A., Mazzei P., De Zotti G., Danese L., 1994, ApJ 427, 140
 Gallimore J.F., Keel W.C., 1993, AJ 106, 1337
 Gautier T.N., Boulanger F., Perault M., Puget J-L., 1992, AJ 103, 1313
 Gregorich D.T., Neugebauer G., Soifer B.T., Gunn J.E., Herter T.L., 1995, AJ 110, 259
 Gronwall C., Koo, D.C., 1995, ApJ 440, L1
 Guiderdoni B., Rocca-Volmerange B., 1991, A&A 252, 435
 Hacking P.B., Houck J.R., 1987, ApJS 63, 311
 Helou G., Soifer B.T., Rowan-Robinson M., 1985, ApJ 298, L7
 Hernquist L., 1989, Nature 340, 687
 Heydon-Dumbleton N.H., Collins C.A., McGillivray H.T., 1989, MNRAS 238, 379
 Huchra E., 1987, in Starbursts and galaxy evolution, (eds. T.X Thuan, T. Montmerle, J. Tran Thanh Van), Editions Frontières, 199
 Hummel E., 1981, A&A 96, 111
 Hutchings J.B., Neff S.G., 1991, AJ 101, 434
 Infante L., Pritchett C.J., 1995, ApJ 439, 565
 Infante L., De Mello D.F., Menanteau F., 1996, ApJ 469, L85
 Larson R.B., Tinsley B.M., 1978, ApJ 219, 46
 Leech K.J., Lawrence A., Rowan-Robinson M., Walker D., Penston M.V., 1988, MNRAS 231, 977
 Leech K.J., Penston M.V., Terlevitch R., Lawrence A., Rowan-Robinson M., Crawford J., 1989, MNRAS 240, 349
 Lilly S.J., Cowie L.L., Gardner J.P., 1991, ApJ 369, 79
 Lilly S.J., 1993, ApJ 411, 501
 Lonsdale C.J., Hacking P.B., 1990, ApJ 339, 712
 Lonsdale C.J., Hacking P.B., Conrow T.P., 1990, ApJ 358, 60
 Lonsdale C.J., Harmon R.T., 1991, in Infrared and radio astronomy, and astrometry, COSPAR 28th Plenary Meeting, 333
 Lonsdale C.J., Chokshi A., 1993, AJ 105, 1333
 Low F.J. et al. , 1984, ApJ 278, L19
 Maccacaro T., Della Ceca R., Gioia I.M., Morris S.L., Stocke J.T., Wolter A., 1991, ApJ 374, 117
 Maddox S.J., Sutherland W.J., Efstathiou G., Loveday J., 1990, MNRAS 243, 692
 Mann R.G., Saunders W., Taylor A.N., 1996, MNRAS 279, 636
 McGaugh S.S., 1994, Nature 367, 538
 McLeod B.A., Rieke M.J., 1995, ApJ 254, 611
 Metcalfe N., Shanks T., Fong R., Jones L.R., 1991, MNRAS 249, 498
 Metcalfe N., Shanks T., Fong R., Roche N., 1995, MNRAS 273, 257
 Minhos J.C., L. Hernquist, 1994, ApJ 431, L9
 Moshir M. et al. , 1992, Explanatory Supplement to the IRAS Faint Source Survey, Version 2, JPL, Pasadena
 Murdoch H.S., Crawford D.F., Jauncey D.L., 1973, ApJ 183, 1
 Oliver S.J., Rowan-Robinson M., Saunders W., 1992, MNRAS 256, 15p
 Oliver S.J., et al. , 1995 in Wide-Field Spectroscopy and the Distant Universe (eds S.J Maddox, A. Aragon-Salamanca), World Scientific, Singapore
 Oliver S.J., Rowan-Robinson M., Broadhurst T.J. et al., 1996, MNRAS 280, 673
 Pearson C., Rowan-Robinson M., 1996, MNRAS 283, 174
 Pence W., 1976, ApJ 203, 39
 Prestage R.M., Peacock J.A., 1983, MNRAS 204, 355
 de Ruiter H.R., Willis A.G., Arp H.C., 1977, A&AS 28, 211
 Rix H.-W., Guhathakurta P., Colless M., Ing K., 1996, MNRAS, submitted

- Rowan-Robinson M., Helou G., Walker., 1987, MNRAS 227, 589
- Rowan-Robinson M., Saunders W., Lawrence A., Leech K., 1991, MNRAS 253, 485
- Rowan-Robinson M., Benn C.R., Lawrence A., McMahon R.G., Broadhurst T.J., 1993, MNRAS 263, 123
- Sanders D.B., Soifer B.T., Elias J.H. et al., 1988, ApJ 325, 74
- Sanders D.B., Soifer B.T., Elias J.H., Neugebauer G., Matthews K., 1988, ApJ 328, L35
- Saunders W., Rowan-Robinson M., Lawrence A., Efstathiou G., Kaiser N., Ellis R.S., Frenk C.S., 1990, MNRAS 242, 318
- Saunders W., Rowan-Robinson M., Lawrence A., 1992, MNRAS 258, 134
- Sauvage M., Thuan T.X., 1994, ApJ 429, 153
- Smail I., Hogg D.W., Yan L., Cohen J.G., 1995, ApJ 449, L105
- Smith B.J., Kleinmann S.G., Huchra J.P., Low F.J., 1987, ApJ 318, 161
- Soifer B.T. et al. , 1987, ApJ 320, 238
- Soneira R.M., Peebles P.J.E., 1978, AJ 83, 845
- Sutherland W., Maddox S.J., Saunders W., McMahon R.G., Loveday J., 1992, MNRAS 248, 483
- Sutherland W., Saunders W., 1992, MNRAS 259, 413
- Taylor C., Brinks E., Grashuis R.M., Skillman E.D., 1995, ApJS 99, 427
- Telles E., Terlevich R., 1995, MNRAS 275, 1
- Toomre A., 1977, in Evolution of Galaxies and Stellar Populations (eds B.M. Tinsley & R.B. Larson), Yale Univ. Obs., New Haven, 401
- Tyson A.J., 1988, AJ 96, 1
- van den Bergh S., Pierce M.J., 1991, ApJ 364, 444
- van den Bergh S., Abraham R.G., Tanvir N.R., Santiago B.X., Ellis R.S., Glazebrook K., 1996, AJ 112, 359
- Wang B., 1991a, ApJ 374, 456
- Wang B., 1991b, ApJ 374, 465
- Wang B., Heckman T.M., 1996, ApJ 457, 645
- Windhorst R.A., Fomalont E.B., Kellermann K.I. et al., 1995, Nature 375, 471
- Wolstencroft R.D., Savage A., Clowes R.G. et al., 1986, MNRAS 223, 279
- Wolstencroft R.D., McGillivray H.T., Lonsdale C.J. et al., 1992, in Digitised Optical Sky Surveys (eds H.T McGillivray & E.B. Thomson), Kluwer, 471
- Zepf S.E., Koo D.C., 1989, ApJ 337, 34